



Give your cells a competitive edge

with the most complete family of xeno-free,
serum-free media for translational research.

Accelerate your product development, scale-up, and cell banking projects with Biological Industries USA's portfolio of xeno-free, serum-free MSC culture systems.

- MSC NutriStem® XF Medium
- PLTGold® Human Platelet Lysate

For more information or to evaluate our systems, apply at www.bioind.com/msc

- High impact culture systems
- Superior cell growth
- cGMP-manufactured
- FDA drug master files
- Used in clinical trials worldwide
- Custom options available

¹Department of Transfusion Medicine and Cell Therapy, Kyoto University Hospital, Kyoto, 606-8507, Japan; ²Department of Hematology and Oncology, Graduate School of Medicine, Kyoto University, Kyoto, 606-8507, Japan; ³Department of Hematology and Oncology, Research Institute for Radiation Biology and Medicine, Hiroshima University, Hiroshima, 734-8553, Japan; ⁴Department of Medicine, Division of Gastroenterology and Hematology, Shiga University of Medical Science, Shiga, 520-2192, Japan; ⁵Department of Cellular and Molecular Biology, Institute of Biomedical & Health Sciences, Hiroshima University, Hiroshima, 734-8553, Japan


*Correspondence: Yasuo Miura, M.D., Ph.D., Department of Transfusion Medicine and Cell Therapy, Kyoto University Hospital, 54 Kawaharacho, Shogoin, Sakyo-ku, Kyoto 606-8507, Japan, Department of Hematology and Oncology, Research Institute for Radiation Biology and Medicine, Hiroshima University, Hiroshima 734-8553, Japan, Tel: +81-75-751-3630, Fax: +81-75-751-4283, E-mail: ym58f5@kuhp.kyoto-u.ac.jp; [§] These senior authors equally contributed to this work.; Grants: This work was supported in part by Grants-in-Aid from the Ministry of Education, Culture, Sports, Science, and Technology of Japan (#15K09453, #16K07171, and #17H04264 to Y.M., T.M., and T.I., respectively) and from the Japan Agency for Medical Research and Development (AMED) (17ek0510022s0601, to T.I.). This work was also supported in part by the Program of the Network-Type Joint Usage/Research Disaster Medical Science of Hiroshima University, Nagasaki University, and Fukushima Medical University (Y.M., S.F., and T.I.).

Received August 24, 2017; accepted for publication December 03, 2017; available online without subscription through the open access option.

©AlphaMed Press
1066-5099/2017/\$30.00/0

This article has been accepted for publication and undergone full peer review but has not been through the copyediting, typesetting, pagination and proofreading process which may lead to differences between this version and the Version of Record. Please cite this article as doi: 10.1002/stem.2759

GVHD amelioration by Human Bone Marrow Mesenchymal Stromal/stem Cell-Derived Extracellular Vesicles is Associated with Peripheral Preservation of Naive T Cell Populations

SUMIE FUJII^{1,2} , YASUO MIURA^{1,3,#}, AYA FUJISHIRO^{1,4}, TAKERO SHINDO², YUTAKA SHIMAZU², HIDEYO HIRAI², HIDETOSHI TAHARA⁵, AKIFUMI TAKAORI-KONDO², TATSUO ICHINOHE^{3,§}, AND TAIRA MAEKAWA^{1,§}

Key words. mesenchymal stem cells • graft-versus-host disease • extracellular vesicles • microRNA • regulatory T cells • naive T cells • hematopoietic stem cell transplantation

ABSTRACT

A substantial proportion of patients with acute graft-versus-host disease (aGVHD) respond to cell therapy with culture-expanded human bone marrow mesenchymal stromal/stem cells (BM-MSCs). However, the mechanisms by which these cells can ameliorate aGVHD-associated complications remain to be clarified. We show here that BM-MSC-derived extracellular vesicles (EVs) recapitulated the therapeutic effects of BM-MSCs against aGVHD. Systemic infusion of human BM-MSC-derived EVs prolonged the survival of mice with aGVHD and reduced the pathologic damage in multiple GVHD-targeted organs. In EV-treated GVHD mice, CD4⁺ and CD8⁺ T cells were suppressed. Importantly, the ratio of CD62L-CD44⁺ to CD62L⁺CD44⁺ T cells was decreased, suggesting that BM-MSC-derived EVs suppressed the functional differentiation of T cells from a naive to an effector phenotype. BM-MSC-derived EVs also preserved CD4⁺CD25⁺Foxp3⁺ regulatory T cell populations. In a culture of CD3/CD28-stimulated human peripheral blood mononuclear cells (PBMCs) with BM-MSC-derived EVs, CD3⁺ T cell activation was suppressed. However, these cells were not suppressed in cultures with EVs derived from normal human dermal fibroblasts (NHDFs). NHDF-derived EVs did not ameliorate the clinical or pathological characteristics of aGVHD in mice, suggesting an immunoregulatory function unique to BM-MSC-derived EVs. Microarray analysis of microRNAs in BM-MSC-derived EVs versus NHDF-derived EVs showed up-regulation of miR-125a-3p and down-regulation of cell proliferative processes, as identified by Gene Ontology enrichment analysis. Collectively, our findings provide the first evidence that amelioration of aGVHD by therapeutic infusion of BM-MSC-derived EVs is associated with the preservation of circulating naive T cells, possibly due to the unique microRNA profiles of BM-MSC-derived EVs. *STEM CELLS* 2017; 00:000–000

SIGNIFICANCE STATEMENT

Cell therapy with human bone marrow mesenchymal stromal/stem cells (BM-MSCs) is clinically effective for patients with intractable acute graft-versus-host disease (aGVHD) after allogeneic hematopoietic stem cell transplan-

tation. This study revealed that BM-MSC-derived extracellular vesicles (EVs) recapitulated the therapeutic effects of BM-MSCs against aGVHD by inhibiting effector T cell induction and preserving peripheral naive T cells. Gene Ontology analysis of microRNAs differentially expressed in BM-MSC-derived EVs suggested that these microRNAs may down-regulate cell proliferative processes. These findings suggest that BM-MSC-derived EVs mediate the anti-aGVHD effects of BM-MSCs, thereby raising the possibility of using EVs as a cell-free therapy for the treatment of aGVHD.

INTRODUCTION

Although molecularly-targeted therapies have improved the prognosis of patients with hematological diseases, allogeneic hematopoietic stem cell transplantation (HSCT) remains the only curative therapy for refractory disease. Acute graft-versus-host disease (GVHD) occurs when immune cells transplanted from a genetically non-identical donor recognize and are activated by alloantigens in HSCT recipients, resulting in organ damage [1]. Various immunosuppressants have been clinically applied for the prevention of acute GVHD [2]. However, a substantial proportion of HSCT recipients develop this potentially life-threatening complication. The efficacy of standard primary therapy with corticosteroids is about 50%, and the complete response rate to secondary therapy with a variety of immunosuppressants is about 30%, with a median overall survival of less than 1 year in steroid-refractory patients [3]. Therefore, development of novel treatment strategies is extremely important to improve the overall survival of recipients of HSCT.

Human mesenchymal stromal/stem cells (MSCs) are multipotent cells that show a variety of biological characteristics, including immunomodulatory capacity [4, 5, 6]. Clinical studies have demonstrated the efficacy of systemic infusion of culture-expanded allogeneic human bone marrow (BM)-MSCs for the treatment of patients with steroid-refractory acute GVHD [7]. In some countries, allogeneic BM-MSC products are clinically used as an off-the-shelf product for steroid-resistant acute GVHD [8]. Previous lines of evidence have suggested that BM-MSCs inhibit the function of immune cells mainly through the local secretion of soluble immune modulators and partially through cell-to-cell contact-dependent mechanisms [9]. However, because most infused BM-MSCs remain in the lungs, these observations do not clearly explain the mechanism by which MSCs can exert “remote” immunomodulatory effects in GVHD-affected organs.

Recently, extracellular vesicles (EVs) have gained interest as mediators of cell-to-cell communication based on their ability to transmit signals to sites of action regardless of physiological barriers [10, 11]. EVs are small membrane particles released from many types of cells. They contain various types of molecules, including microRNAs that regulate a diverse range of biological pro-

cesses [12]. Several studies have demonstrated that BM-MSC-derived EVs contribute to the immunomodulatory and regenerative effects of MSCs [13]. Most of these reports show that MSC-derived EVs can recapitulate the therapeutic and regenerative effects of MSCs on damaged tissues/organs in models of myocardial ischemia [14], acute tubular injury [15], stroke [16], acute lung injury/ischemia [17, 18], and skin wounds [19]. More recently, a case report described the successful treatment of a patient with refractory acute GVHD by intravenous infusions of EVs derived from BM-MSCs [20]. However, the biologic mechanisms by which BM-MSC-derived EVs exert these functions remain unknown.

In this study, we examined the effects of human BM-MSC-derived EVs on the clinical, pathological, and immunologic characteristics of acute GVHD model mice. A microarray analysis was also conducted to evaluate the biological processes mediated by microRNAs within human BM-MSC-derived EVs.

MATERIALS AND METHODS

Human BM-MSC culture

Human MSCs were isolated from BM samples purchased from AllCells (Alameda, CA) using our previously published method [21, 22]. BM samples were obtained from three different healthy adult donors. A single-cell suspension of 1×10^6 BM mononuclear cells was seeded into a 15 cm culture dish, and adherent cells were cultured in Advanced Minimal Essential Medium (Invitrogen/Thermo Fisher Scientific, Waltham, MA) supplemented with 5% fetal bovine serum (FBS; Gibco/Thermo Fisher Scientific), 100 μ M ascorbic acid (Wako Pure Chemical Industries, Osaka, Japan), 2 mM L-glutamine, 100 U/mL penicillin, and 100 μ g/mL streptomycin (all from Gibco/Thermo Fisher Scientific) (complete culture medium, CCM). Primary cultures were passaged to disperse the colony-forming cells (passage 1). Cells at passage 3 were used as BM-MSCs in this study. Prior to use in experiments, surface marker expression profiles of these cells were obtained to confirm that the cells fulfil the minimal definition criteria for human MSCs, as proposed by the International Society for Cellular Therapy [23]. In addition, the multilineage differentiation capacity and hematopoiesis-inducing capacity of these cells were confirmed as previously

described [24, 25]. In some experiments, normal human dermal fibroblasts (NHDFs) purchased from Lonza (Basel, Switzerland) were cultured using the FGM-2 Bullkult Kit (Lonza), which contains human fibroblast growth factor- β , insulin, FBS, and gentamicin/amphotericin-B.

EV preparation

Human BM-MSCs (2×10^5 cells) were plated in T-75 culture flasks in CCM. Seven days later, the CCM was replaced with 10 mL serum-free medium (SFM). The conditioned SFM was collected after 24 hours and centrifuged at $2,000 \times g$ for 30 minutes. The supernatant fraction was passed through a $0.2 \mu\text{m}$ filter, mixed with Total Exosome Isolation Reagent (Invitrogen/Thermo Fisher Scientific), incubated overnight at 4°C , and centrifuged at $10,000 \times g$ for 1 hour. The EV-containing pellet was resuspended in Dulbecco's phosphate-buffered saline (DPBS) at $100 \mu\text{L}$ per 1.0×10^6 BM-MSCs. The particle and protein contents of the EVs were measured by tunable resistive pulse sensing (qNano, Izon Science Ltd, Oxford, United Kingdom) [26] or by Bradford protein assay (Thermo Fisher Scientific), respectively. The mean protein and particle contents of the EV preparations were 4.48 mg/mL and 4.23×10^9 particles/mL, respectively.

Immunoblot analysis and transmission electron microscopy

For immunoblot analysis, EVs solutions were lysed with 5X SDS sample buffer, separated on 4–12% SDS-PAGE gels (Invitrogen/Thermo Fisher Scientific), and transferred to PVDF membranes. Primary antibodies against CD63 (clone TS63, Abcam, London, UK) and CD81 (rabbit polyclonal, System Biosciences, Palo Alto, CA) were used to detect EVs. For transmission electron microscopy, EVs were placed on formvar-coated copper grids and allowed to absorb onto the grid overnight. After the excess solution was carefully removed using filter paper, the samples were stained with 1% uranyl acetate for 10 minutes, dried, and observed with a JEOL JEM-1230S transmission electron microscope operating at 80 KV (JEOL, Tokyo, Japan).

In vitro T cell expansion assay

Human peripheral blood mononuclear cells (PBMCs) were separated using Ficoll-Paque Plus (GE Healthcare Japan, Tokyo, Japan). PBMCs (1×10^6 /per well) were activated with anti-CD3 and anti-CD28 antibodies using Human T-Activator CD3/CD28 Dynabeads (Life Technologies/Thermo Fisher Scientific) in 24-well plates ($25 \mu\text{L}$ /well) according to the manufacturer's instructions (day 0). Five days later (day 5), the number of cells was counted by Trypan blue dye exclusion and their surface marker expression was assessed by flow cytometry. For co-culture assays, BM-MSCs (5×10^4 /well) were prepared in 24-well plates the day before adding the PBMCs (day -1). To examine the effects of EVs, $5 \mu\text{L}$ EVs

prepared from conditioned SFM derived from 5×10^4 BM-MSCs was added to the T cell expansion culture.

Murine acute GVHD model

Specific pathogen-free 7–9-week-old C57BL/6 mice (H-2D^b), DBA/2 mice (H-2D^d), and B6D2F1 mice (C57BL/6 \times DBA/2 F1; H-2D^{bxd}) were obtained from CLEA Japan (Tokyo, Japan). For induction of GVHD, 1×10^7 spleen cells from parental C57BL/6 mice (B6) were intravenously injected via the tail vein into B6D2F1 (BDF1) mice that received 8 Gy total body irradiation prior to transplantation [27]. GVHD was indicated by a $\geq 10\%$ loss of body weight in the recipient mice [28]. The GVHD mice were randomized into two groups 5 days after the injection of the spleen cells. The control group received a tail vein injection of $200 \mu\text{L}$ saline, and the EV-treated mice received an injection of $200 \mu\text{L}$ saline containing EVs derived from 2×10^6 human BM-MSCs per kg of body weight; e.g., for a mouse weighing 20 g, $4 \mu\text{L}$ EVs derived from 4×10^4 human BM-MSCs were prepared and adjusted to a final volume of $200 \mu\text{L}$ with saline (approximately 1.6×10^7 particles containing $16 \mu\text{g}$ protein). The study was approved by the Committee for Animal Research of the Kyoto University Graduate School of Medicine (Medkyo #17284). All animal studies were performed in accordance with the relevant guidelines and regulations.

Histological and clinical assessment of GVHD

For histological assessment, mice were sacrificed 6 days after administration of EVs, and tissue samples from the large bowel, liver, small bowel, and skin were collected. The severity of GVHD was scored by evaluating hematoxylin and eosin (HE)-stained paraffin-embedded sections of these tissues/organs, as previously described [29]. Seven (for the large and small bowel) or ten (for the liver) parameters were evaluated and scored as follows: 0 (normal), 0.5 (rare, focal), 1 (mild, focal), 2 (mild, diffuse), 3 (moderate, diffuse), or 4 (severe, diffuse). Scores from each parameter were summed for a total score of 0–28 for the large bowel and small bowel, and 0–40 for the liver. For evaluation of the skin, the severity of damage was evaluated as mild, moderate, or severe by previously described criteria, with some modifications [30]. Clinical assessment was performed 10 days after the injection of spleen cells and was based on five parameters, including weight loss, posture, activity, fur texture, and skin integrity, as previously described [28, 31]. A score of 0 (good) to 2 (poor) for each parameter was summed, for a total score of 0–10.

Flow cytometric analysis

For the analysis of surface marker expression of BM-MSCs, NHDFs, and murine PB, a single-cell suspension of these cells was stained with fluorescent-conjugated antibodies and analyzed on a FACS Canto II (BD Biosciences, Franklin Lakes, NJ). For the analysis of expanded cells in anti-CD3/CD28-stimulated human PBMC cul-

tures, the Dynabeads were removed with a magnet prior to staining. The primary antibodies used in this study are listed in Table S1. Dead cells were excluded by staining with propidium iodide. For the staining of the intracellular protein Foxp3, the Live/Dead Fixable Blue Dead Cell Stain Kit (Molecular Probes/Thermo Fisher Scientific) was used to exclude dead cells. Data were analyzed using FlowJo software (Tree Star, Ashland, OR). The CD3-negative population, as determined by the staining of the isotype control Ab, included few CD4⁺/CD8⁺ cells.

Microarray analysis of microRNAs

Total RNA was extracted from human BM-MSC- or NHDF-derived EVs using the miRNeasy Mini Kit (Qiagen, Hilden, Germany). The integrity of the RNA was evaluated using an Agilent 2100 Bioanalyzer (Agilent Technologies, Santa Clara, CA). The extracted total RNA was labeled with Cyanine5 using the 3D-Gene miRNA labeling kit (Toray Industries, Kamakura, Japan). The microRNA expression profiles were examined using the 3D-Gene miRNA microarray analysis system (Toray Industries). The mRNA targets of microRNAs were predicted using TargetScan (<http://www.targetscan.org/>). Gene Oncology (GO) enrichment and Kyoto Encyclopedia of Genes and Genomes (KEGG) pathway analyses were performed using GeneCodis tools with the predicted targets of each microRNA as the input (<http://genecodis.cnb.csic.es/>). The complete microarray data are available in the NCBI Gene Expression Omnibus (GEO). The microarray accession number is GSE99082.

Array analysis of soluble factors

Soluble factors expressed by human BM-MSC- or NHDF-derived EVs were analyzed using the Proteome Profiler Human Cytokine Array (R&D Systems, Minneapolis, MN) according to the manufacturer's instructions. EVs were solubilized in Tween 20 (MP Biomedicals, Illkirch-Graffenstaden, France) at a final concentration of 1% and sonicated for 60 seconds. Protein prepared from EVs (300 µg) was mixed with a cocktail of biotinylated detection antibodies and applied to membranes coated with immobilized capture antibodies. Immunoreactive proteins were detected and visualized with streptavidin-horseradish peroxidase and chemiluminescent detection reagents. Protein expression levels were measured using Quantity One software (Bio-Rad, Hercules, CA).

Statistical analysis

Fisher's exact test was used unless otherwise indicated. Bar graphs indicate the mean ± SD. Statistical significance is expressed as follows: *, $P < 0.05$; **, $P < 0.01$. Survival was estimated using the Kaplan–Meier method, and survival estimates were compared by log-rank testing. Statistical analyses were performed with the EZR software program [32].

RESULTS

Characteristics of EVs and their originated human BM-MSCs

An overview of EV preparation from culture supernatants of human BM-MSCs is shown in Fig. S1A. EVs from three different lots of BM-MSCs expressed the EV-associated markers CD63 and CD81 by immunoblot analysis (Fig. S1B). Transmission electron microscopy of the prepared EVs identified particles with a saucer-like morphology, as previously described [33, 34] (Fig. S1C). The size of the particles in the EV preparations ranged from 90 to 400 nm, with most particles measuring approximately 110 nm (Fig. S1D).

When human PBMCs were stimulated with anti-CD3 and anti-CD28 antibodies in the presence of human BM-MSCs, the number of expanded cells at 5 days was significantly lower than in cultures of PBMCs stimulated alone (Fig. 1A, B). Flow cytometric analysis showed that the expansion of total T cells as well as CD4⁺T cells was substantially suppressed (Fig. 1C–E). This suppressive effect was also observed when activated PBMCs were co-cultured with different lots of BM-MSCs and when a different lot of activated PBMCs was co-cultured with the BM-MSCs (Fig. S2A, B). The PBMCs and MSCs were mismatched by at least six out of eight human leukocyte antigen (HLA) alleles (Table S2). Therefore, BM-MSC lots used in this study could suppress the expansion of T cells in an HLA-independent manner, as previously demonstrated [6, 35].

Human BM-MSC-derived EVs suppress the expansion of effector T cells but preserve naive regulatory T cells *in vitro*

The effect of EVs on the expansion of functional T cell subsets was evaluated in cultures of anti-CD3/CD28-stimulated PBMCs. In the presence of human BM-MSC-derived EVs, the expansion of anti-CD3/CD28-stimulated human PBMCs was suppressed (Fig. 1A, B). The expansion of total T cells, including CD4⁺ T cells, was suppressed in a manner similar to co-cultures with BM-MSCs (Fig. 1C–E). The expansion of CD8⁺ T cells was also suppressed in the presence of EVs, but not in co-cultures with BM-MSCs (Fig. 1C–E). When the supernatant fraction generated in the process of EV preparation was used instead of EVs in the expansion cultures, these suppressive effects were not observed (Fig. S1A, E, F). The EV-mediated suppressive effects were observed when anti-CD3/CD28-stimulated PBMCs were cultured in the presence of different lots of BM-MSC-derived EVs (Fig. S2A), and when different lots of PBMCs were cultured in the presence of BM-MSC-derived EVs (Fig. S2B).

Previous studies suggested that regulatory T cells (Treg) may be associated with the immunomodulatory functions of BM-MSCs [6]. We therefore examined whether BM-MSC-derived EVs influence Treg. In the anti-CD3/CD28-stimulated PBMC expansion cultures, the frequency of CD45RA⁺Foxp3^{low} naive Treg (Fraction

1) was higher, and the frequency of CD45RA-Foxp3^{high} effector Treg (Fraction 2) was lower, in the presence of EVs (Fig. 1F, G). In addition, the ratio of total CD8+ T cells to naive Treg was lower in the presence of EVs (Fig. 1F, G). Finally, the frequency of CD45RA-Foxp3^{low} non-Treg (Fraction 3) was lower in cultures with EVs compared to cultures of PBMCs alone, suggesting the suppression of non-Treg within the Foxp3-expressing T cell population by BM-MSC-derived EVs. Collectively, these data demonstrate that BM-MSC-derived EVs preserve naive Treg.

With regards to other hematopoietic cell populations, the frequency of CD19+ cells, CD3-CD56+ cells, CD3-CD16+ cells, CD11b+ cells, and CD3-CD4^{dim} cells remained high in the expansion cultures of PBMCs containing EVs (Fig. S3). These results suggested that EVs specifically suppress the expansion of T cells, but not B cells, NK cells, or mature myeloid cell populations. In particular, B cells and mature myeloid cell populations seemed to be preserved in the expansion cultures with EVs (Fig. S3).

Human BM-MSC-derived EVs ameliorate the clinical and pathological characteristics of acute GVHD in mice

To investigate the effects of BM-MSC-derived EVs on acute GVHD *in vivo*, a major histocompatibility complex (MHC)-haploidentical murine model was used in which 1×10^7 spleen cells from C57BL/6 mice (B6, H-2D^b) were injected into B6D2F1 (BDF1, H-2D^{bxd}) mice. These mice were randomly divided into two groups 5 days after the injection of spleen cells. One group of GVHD mice was treated with human BM-MSC-derived EVs, and the other group of mice received saline injections (Fig. 2A). GVHD mice that received systemic infusion of EVs showed prolonged survival, with a median survival of 16 days compared with 10 days in the control GVHD mice (Fig. 2B). The clinical scores of EV-treated mice were lower than those of the control mice (average of 2.8 versus 3.5, Fig. 2C), indicating that EVs ameliorated the systemic symptoms of acute GVHD such as body weight loss. EV treatment also significantly mitigated GVHD-associated pathology in the large bowel, particularly the infiltration of the lamina propria by inflammatory cells and the vacuolization and attenuation of surface colonocytes (Fig. 2D–F). The histological scores of the livers of the EV-treated GVHD mice were lower than those of the control mice, but this did not reach statistical significance, and the histological scores of the small bowels of the EV-treated mice were comparable to those of the control mice (Fig. 2D, S4B, Table S3). With regards to the skin, the percentage of mice with severe damage was lower in the EV-treated group than in the control group (60.0% versus 88.8%) (Fig. 2G, S4B, Table S4). Collectively, systemic administration of human BM-MSC-derived EVs significantly prolonged the survival of mice with acute GVHD, which was accompanied by an amelioration of clinical GVHD symptoms and pathologi-

cal damage in multiple GVHD-targeted organs, particularly the large bowel.

Human BM-MSC-derived EVs suppress the functional differentiation of T cells in mice with GVHD

PB T cell subsets were analyzed in GVHD mice that received systemic administration of EVs. Flow cytometric analysis indicated that the expansion of CD8+ T cells was suppressed by treatment with human BM-MSC-derived EVs (Fig. 3A, B). In the control GVHD mice, most of the CD8+ and CD4+ T cells were CD62L-CD44+ effector T cells (Fig. 3C, S5B, D). In GVHD mice treated with EVs, the frequency and number of effector T cells among CD4+ and CD8+ T cells were decreased, and conversely, the frequency and number of CD62L+CD44-naive T cells were increased (Fig. 3C, S5A–D). These results suggest that systemic administration of human BM-MSC-derived EVs suppressed the functional differentiation of T cells from a naive phenotype to an effector phenotype. The frequency of CD4+CD25+Foxp3+ Treg was also decreased in the GVHD control mice compared to mice without GVHD, whereas the EV-treated GVHD mice contained a substantial CD4+CD25+Foxp3+ population (Fig. 3D), suggesting that human BM-MSC-derived EVs preserve Treg.

The populations of non-T cells, including CD19+Gr-1- cells (B cells), Gr-1-CD11b+ cells (monocytes), and Gr-1+CD11b+ cells (neutrophils), were depleted in the control GVHD mice compared to mice without GVHD, but EV treatment ameliorated the depletion of these cell populations (Fig. S6).

NHDF-derived EVs do not suppress T cell expansion *in vitro* or ameliorate acute GVHD in mice

We explored whether the anti-GVHD effects of BM-MSC-derived EVs could be induced by EVs derived from other stromal cells. To address this, we used NHDFs because they are adherent stromal cells with a similar morphology to human BM-MSCs. Flow cytometric analysis showed that NHDFs were negative for hematopoietic and endothelial markers, including CD45, CD34, CD11b, CD19, CD31, and HLA-DR, and were positive for mesenchymal stem cell-associated markers, including CD105, CD73, CD90, CD44, and CD166, which was a similar expression pattern as BM-MSCs (Fig. S7A, B). On the other hand, NHDFs were distinct from BM-MSCs in the expression of CD10, CD106, and CD146 (Fig. S8A). In addition, NHDFs did not show apparent multi-differentiation capability to osteogenic (Fig. S8B, C), chondrogenic (Fig. S8D), or adipogenic (Fig. S8E, F) cells *in vitro*. Moreover, unlike BM-MSCs, NHDFs did not form bone or induce hematopoietic marrow when subcutaneously transplanted into immunocompromised mice (Fig. S8G). Thus, NHDFs were fundamentally different from BM-MSCs.

When anti-CD3/CD28-stimulated human PBMCs were cultured with NHDF-derived EVs, the expansion of total T cells, including CD4⁺ and CD8⁺ T cells, was comparable to that in cultures of PBMCs alone and in cultures with the supernatant fraction generated in the process of EV preparation from conditioned SFM of NHDFs (Fig. S9A, B). Therefore, NHDF-derived EVs did not have the suppressive effects on T cells seen with BM-MSC-derived EVs.

In accordance with these observations, when MHC-haploidentical GVHD mice received NHDF-derived EVs, the survival of the mice was not prolonged and was actually shortened compared to the control mice (Fig. S10A). The clinical scores of the GVHD mice treated with NHDF-derived EVs were comparable to those of the control GVHD mice (Fig. S10B). In addition, the histological scores for the large bowel, liver, and small bowel of GVHD mice treated with NHDF-derived EVs were comparable to those of the control GVHD mice (Fig. S10C). With regards to the skin, in the mice treated with NHDF-derived EVs, the percentage of mice with severely damaged skin was lower, and conversely, the percentage of mice with mildly or moderately damaged skin was higher compared to the control mice (Fig. S10D). Flow cytometric analysis of PB T cell subsets in GVHD mice indicated that the expansion of CD8⁺ T cells was not suppressed by treatment with NHDF-derived EVs (Fig. S10E). In addition, the frequency of effector T cells, naive T cells, and Treg in GVHD mice treated with NHDF-EVs was comparable to that in the control GVHD mice (Fig. S10E, F). Collectively, these data indicate that systemic administration of NHDF-derived EVs had no significant effect on the functional differentiation of T cells from a naive phenotype to an effector phenotype or on the preservation of Treg. These data suggest that the immunologic and anti-GVHD effects of human BM-MSC-derived EVs are unique, at least in comparison to NHDF-derived EVs.

Proliferation-related gene signatures are down-regulated by microRNAs in human BM-MSC-derived EVs

The expression of multiple soluble factors such as cytokines, chemokines, and growth factors in NHDF-derived and BM-MSC-derived EVs was compared (Fig. S11). Differences in the expression of several molecules, including macrophage migration inhibiting factor (MIF), interleukin (IL)-13, plasminogen activator inhibitor (PAI)-1, and CXCL12, were observed.

Finally, microarray analysis of microRNAs in BM-MSC-derived EVs was performed (Fig. S12). This analysis identified 336 and 337 microRNAs that were up- or down-regulated, respectively, in human BM-MSC-derived EVs compared to NHDF-derived EVs (Fig. 4A, S-File 1). Among them, miR-125a-3p was identified as the most highly up-regulated microRNA in BM-MSC-derived EVs (Fig. 4B). TargetScan analysis predicted 11726 mRNAs as targets of the top ten up-regulated mi-

croRNAs (S-File 2). Among them, 3477 mRNAs were commonly targeted by three or more microRNAs and were selected for further analysis. GO enrichment analysis showed that these commonly targeted genes were highly involved in the regulation of proliferation-related processes (Table 1). A similar analysis was performed on 12553 mRNAs that were predicted as targets of the top ten down-regulated microRNAs (Fig. 4B, S-File 3). Among them, 4356 mRNAs were commonly targeted by three or more microRNAs, and these mRNAs were found to be highly involved in inhibition of proliferation by GO enrichment analysis (Table 1). Collectively, these analyses suggest that microRNAs within BM-MSC-derived EVs down-regulate cell proliferation. Furthermore, KEGG pathway analysis identified gene groups involved in cell cycle regulation, T cell receptor signaling, and GVHD (Fig. 4C). These pathways were considered to be down-regulated because they include genes targeted by commonly up-regulated microRNAs.

DISCUSSION

A series of clinical studies have examined the efficacy of systemic infusion of culture-expanded BM-MSCs for acute GVHD patients and shown overall response rates ranging from about 30% to 80% [36, 37]. Attempts to improve the outcome of BM-MSC therapy have been based on the concept that this form of therapy is dependent on the number of infused cells that can successfully traffic to sites of damaged or diseased tissue [38]. However, systemic administration of an increased number of cells did not augment the therapeutic effects of BM-MSCs in GVHD [39]. In addition, another approach, in which BM-MSCs were directly delivered into the gut via the mesenteric artery, was not more effective than systemic injection [40]. These clinical results underscore the current molecular understanding that the therapeutic effects of BM-MSCs are, at least in acute GVHD, attributed mainly to secreted immunomodulatory factors [9, 41]. In the present study, we found, for the first time, that human BM-MSC-derived EVs ameliorated GVHD symptoms and pathology in GVHD-targeted organs, and prolonged the survival of GVHD mice in association with preservation of circulating naive T cell populations.

BM-MSCs suppress the expansion of human naive T cells as well as activated CD4⁺ and CD8⁺ T cells regardless of major histocompatibility complex compatibility [41, 42]. It has also been reported that BM-MSCs induce human Treg, which inhibit allogeneic lymphocyte proliferation [43, 44]. In line with these reports, we found that BM-MSC-derived EVs suppressed the proliferation of CD4⁺ and CD8⁺ T cells in anti-CD3/CD28-stimulated expansion cultures of human PBMCs and in PB obtained from the GVHD mice. In addition, BM-MSC-derived EVs suppressed the functional differentiation of T cells from a naive to an effector phenotype in the GVHD mice. Moreover, naive Treg were preserved in the presence of BM-MSC-derived EVs in cultures of anti-CD3/CD28-

stimulated human PBMCs and in PB of the GVHD mice. Collectively, it is conceivable that the anti-GVHD effect of BM-MSCs is, at least partially, associated with an EV-mediated immunomodulatory effect on T cells.

However, a number of studies suggest that MSC-derived EVs mimic the therapeutic effects of their MSCs of their origin to a large extent, even though the underlying mechanisms may not necessarily be similar [13]. In our *in vitro* study, BM-MSCs suppressed the expansion of CD3⁺ T cells to a lesser extent than EVs derived from the same number of the BM-MSCs from which they originated. BM-MSC-derived EVs may, therefore, have a stronger effect on T cell suppression than BM-MSCs. This is supported by the observation that the suppressive effect of EVs on T cell expansion was dose-dependent (data not shown). With respect to the Foxp3-expressing T cell population, the suppression of CD45RA-Foxp3^{low} cells (non-Treg) by BM-MSC-derived EVs might reflect the suppression of activated CD4⁺ T cells. Given that CD45RA-Foxp3^{low} naive Treg become CD45RA-Foxp3^{high} Treg upon anti-CD3/CD28 stimulation, it is possible that BM-MSC-derived EVs had the enhanced suppressive effect on the ability of Treg to shift from a naive to an activated status or that BM-MSC-derived EVs induced more naive Treg within the CD4⁺ T cell population compared to BM-MSCs. Previous *in vitro* studies on the modulation of functional T cell populations by BM-MSCs have been contradictory [45, 46, 47]. As for *in vivo* studies, a recent report suggested that EVs contribute to the suppression of Th1 cells in a human-to-mouse xenogeneic chronic GVHD model [48]. Further studies are needed to determine the contribution of EVs to the BM-MSC-mediated T cell modulation.

Various types of cells release EVs. To address the unique effects of human BM-MSC-derived EVs, we used NHDF-derived EVs as a control because human BM-MSCs and fibroblasts share many properties, including a plastic-adherent spindle-like morphology and a similar surface marker expression profile [49]. Nevertheless, NHDFs are functionally different from BM-MSCs. In our analysis, NHDFs lacked multi-differentiation capacity and hematopoiesis induction. In addition, NHDF-derived EVs did not suppress T cell expansion in cultures with anti-CD3/CD28-stimulated PBMCs. Most importantly, NHDF-derived EVs did not exhibit the anti-GVHD effects of BM-MSC-derived EVs, including amelioration of clinical symptoms, resolution of the pathology in the gut and liver, or prolongation of survival. These results suggest that BM-MSC-derived EVs have a unique therapeutic effect in acute GVHD. Interestingly, systemic infusion of human BM-MSC-derived EVs was effective in resolving the pathology in the large bowel and skin of the GVHD mice. This is consistent with the clinical characteristics of BM-MSC therapy for acute GVHD [7, 8, 50, 51]. The mechanisms that underlie the differences in the efficacy of BM-MSC-derived EVs among organs/tissues have not been well-studied.

There are limitations to this study. First, the effects of BM-MSC-derived EVs on GVHD-targeted organs were

modest. Only the suppression of GVHD pathology in the large intestine was significantly associated with clinical improvement in GVHD mice treated with BM-MSC-derived EVs. Although multiple organs can be affected in GVHD, pathologic damage to the large intestine can be lethal; therefore, favorable effects of BM-MSC-derived EVs on the large intestine might predominantly contribute to the improved clinical outcomes. Second, the survival of GVHD mice treated with NHDF-derived EVs was less than that of the control GVHD mice, despite the lack of effects on PB T cells. This suggests the possibility that the distribution of T cell subsets in the PB does not reflect the distribution in GVHD-targeted organs.

Comprehensive characterization of EVs would provide the information necessary to explore their therapeutic potential [52]. A previous study by Phinney et al. reported the microRNA expression profiles of MSC-derived exosomes [53]. Because they compared microRNA expression levels between exosomes and their parental MSCs, the most highly up- or down-regulated microRNAs were different from the most highly regulated microRNAs in our analysis. However, it is of interest that such microRNAs in that study were also up-regulated in EVs in our analysis. MicroRNAs that are expressed differentially in EVs compared with the parental MSCs might contribute to MSC-associated functions.

Microarray analysis of microRNAs in BM-MSC-derived EVs versus NHDF-derived EVs revealed the differential expression of multiple microRNAs, suggesting the involvement of multiple biological processes. Previous studies have demonstrated that BM-MSCs inhibit the proliferation of activated T cells via cell cycle arrest [54, 55] and modulate the expression of various cytokines, including proinflammatory (e.g., IL-2, IFN- γ , TNF- α) and anti-inflammatory cytokines (e.g., IL-4, IL-10), which play important roles in the pathogenesis of acute GVHD [6, 9, 56, 57, 58, 59]. The GO enrichment analysis identified the down-regulation of multiple cell proliferation-related processes but not altered production of these cytokines. Furthermore, KEGG analysis suggested the down-regulation of pathways associated with GVHD and T cell receptor signaling. These comprehensive analyses support our *in vitro* and *in vivo* results, where T cell expansion was suppressed by BM-MSC-derived EVs and acute GVHD was suppressed clinically and pathologically in GVHD mice.

Of the microRNAs that were differentially expressed in human BM-MSC-derived EVs and NHDF-derived EVs, miR-125a-3p was the most highly altered microRNA. Notably, miR-125a-3p suppressed cell proliferation in several cell lines, consistent with our *in vitro* observations [60, 61, 62]. It has also been shown that miR-125a is down-regulated in PBMCs from patients with systemic lupus erythematosus (SLE) [63]. The down-regulation of miR-125a contributed to the elevated expression of the inflammatory chemokine regulated upon activation, normal T cell expressed and secreted (RANTES) by tar-

getting Kruppel-like factor 13 (KLF13) in activated T cells [64]. Therefore, the up-regulation of miR-125a-3p in BM-MSC-derived EVs might contribute to the suppression of T cells. Collino et al. performed microarray analysis of microRNAs contained in EVs released from both BM-MSCs and liver-resident stem cells [65]. Although miR-125a was not specifically discussed by the authors, it was one of the most abundantly expressed microRNAs in microvesicles and their cells of origin. Their analysis indicated that abundantly expressed microRNAs in BM-MSCs contributed to multiple cell processes, including regulation of the immune system, differentiation-related functions, and processes related to the regulation of cell cycle progression, proliferation, and cell death. One microRNA can regulate many target genes, while conversely one gene can be targeted by many microRNAs; thus multiple relationships between microRNAs and target genes elaborately determine the fate of T cells. It will be important to use a conditional microRNA-125a-3p knockout mouse model to more conclusively demonstrate the association between up-regulated microRNA-125a-3p and the anti-GVHD effect.

Array analysis of multiple soluble factors identified several molecules that were more highly expressed in BM-MSC-derived EVs than in NHDF-derived EVs. Among them, CXCL12 could potentially be associated with the amelioration of GVHD, as was reported in a previous study [66]. EVs contain a variety of bioactive molecules, and further analysis of immune-modulatory factors is warranted to fully understand the anti-GVHD mechanism of BM-MSC-derived EVs.

Use of BM-MSC-derived EVs may have potential advantages over their cell of origin in some aspects. From a safety standpoint, concerns about the transformation of BM-MSCs to malignant cells in patients do not need to be considered with the use of EVs. From a therapeutic standpoint, BM-MSCs may become trapped in capillaries, particularly in the lungs, and become unable to reach damaged or diseased tissues/organs, which is necessary for them to exert their therapeutic effects. This is also not a concern with EVs. On the other hand, BM-MSCs are activated by proinflammatory cytokines present in the microenvironment of damaged or diseased tissues/organs [67]. This implies that the immunomodulatory effects of BM-MSCs might not be exerted in the absence of abnormal environmental conditions. Our study suggests that BM-MSC-derived EVs have therapeutic effects in acute GVHD. However, the EVs showed strong suppression of T cell activation *in vitro*, and extreme immunosuppression by BM-MSC-derived EVs may increase susceptibility to infection in a clinical setting. In addition, because EVs are small, spherical membrane fragments and may include exosomes, microvesicles, and apoptotic bodies [68], there is a possibility that the BM-MSC-derived EV-

concentrated fractions in this study contain the above particles [69]. Therefore, additional research incorporating more homogenous EV preparations is warranted.

CONCLUSION

Human BM-MSC-derived EVs exerted immunomodulatory effects on T cells *in vitro* and anti-GVHD effects in mice. Amelioration of acute GVHD by BM-MSC-derived EVs was associated with the preservation of circulating naive T cells. Microarray analysis identified microRNAs associated with the immunomodulatory effects of BM-MSC-derived EVs. Further studies are needed to increase the potency of BM-MSC-derived EVs and to better understand the mechanisms of action of this novel potential therapeutic for acute GVHD.

ACKNOWLEDGMENTS

The authors thank Ms. Yoko Nakagawa (Kyoto University) and Ms. Ikuko Fukuba (Hiroshima University) for their excellent technical assistance. The authors also thank Drs. Mariko Ikuo and Shigeyuki Teranishi (Hiroshima University) for their EV analysis.

AUTHOR CONTRIBUTIONS

S.F.: Conception and design, collection of study material, collection and assembly of data, data analysis and interpretation, manuscript writing.; Y.M.: Conception and design, financial support, collection of study material, collection and assembly of data, data analysis and interpretation, manuscript writing.; A.F., T.S., Y.S.: Conception and design, collection of study material, collection and assembly of data, data analysis and interpretation, manuscript writing.; H.H.: Conception and design, collection of study material, assembly of data, data analysis and interpretation, manuscript writing.; H.T.: Collection and assembly of data, data analysis and interpretation.; A.T.-K., T.I., T.M.: Conception and design, financial support, administrative support, provision of study material, data analysis and interpretation, manuscript writing.; All authors approved the final version of the manuscript.

DISCLOSURE OF POTENTIAL CONFLICTS OF INTEREST

Hideyo Hirai received research funding from Kyowa Hakko Kirin and Novartis Pharma. Hidetoshi Tahara is a founder and the chairman/chief executive officer of MiRTel Co. LTD., and owns stock in MiRTel Co. LTD. Taira Maekawa received research funding from Bristol-Meyers Squibb. The remaining authors have no conflicts of interest to declare.

REFERENCES

- 1 Blazar BR, Murphy WJ, and Abedi M. Advances in graft-versus-host disease biology and therapy. *Nat Rev Immunol* 2012;12:443–458.
- 2 Deeg HJ. How I treat refractory acute GVHD. *Blood* 2007;109:4119–4126.
- 3 Martin PJ, Rizzo JD, Wingard JR et al. First- and second-line systemic treatment of acute graft-versus-host disease: recommendations of the American Society of Blood and Marrow Transplantation. *Biol Blood Marrow Transplant* 2012;18:1150–1163.
- 4 Lazarus HM, Haynesworth SE, Gerson SL et al. Ex vivo expansion and subsequent infusion of human bone marrow-derived stromal progenitor cells (mesenchymal progenitor cells): implications for therapeutic use. *Bone Marrow Transplant* 1995;16:557–564.
- 5 Pittenger MF, Mackay AM, Beck SC et al. Multilineage potential of adult human mesenchymal stem cells. *Science* 1999;284:143–147.
- 6 Aggarwal S and Pittenger MF. Human mesenchymal stem cells modulate allogeneic immune cell responses. *Blood* 2005;105:1815–1822.
- 7 Le Blanc K, Frasson F, Ball L et al. Mesenchymal stem cells for treatment of steroid-resistant, severe, acute graft-versus-host disease: a phase II study. *Lancet* 2008;371:1579–1586.
- 8 Muroi K, Miyamura K, Okada M et al. Bone marrow-derived mesenchymal stem cells (JR-031) for steroid-refractory grade III or IV acute graft-versus-host disease: a phase II/III study. *Int J Hematol* 2016;103:243–250.
- 9 Le Blanc K and Mougiakakos D. Multipotent mesenchymal stromal cells and the innate immune system. *Nat Rev Immunol* 2012;12:383–396.
- 10 Raposo G and Stoorvogel W. Extracellular vesicles: exosomes, microvesicles, and friends. *J Cell Biol* 2013;200:373–383.
- 11 Pitt JM, Kroemer G, and Zitvogel L. Extracellular vesicles: masters of intercellular communication and potential clinical interventions. *J Clin Invest* 2016;126:1139–1143.
- 12 EL Andaloussi S, Mäger I, Breakefield XO et al. Extracellular vesicles: biology and emerging therapeutic opportunities. *Nat Rev Drug Discov* 2013;12:347–357.
- 13 Phinney DG and Pittenger MF. Concise Review: MSC-derived exosomes for cell-free therapy. *Stem Cells* 2017;35:851–858.
- 14 Lai RC, Arslan F, Lee MM et al. Exosome secreted by MSC reduces myocardial ischemia/reperfusion injury. *Stem Cell Res* 2010;4:214–222.
- 15 Bruno S, Grange C, Deregibus MC et al. Mesenchymal stem cell-derived microvesicles protect against acute tubular injury. *J Am Soc Nephrol* 2009;20:1053–1067.
- 16 Doeppner TR, Herz J, Görgens A et al. Extracellular vesicles improve post-stroke neuroregeneration and prevent posts ischemic immunosuppression. *Stem Cells Transl Med* 2015;4:1131–1143.
- 17 Lee C, Mitsialis SA, Aslam M et al. Exosomes mediate the cytoprotective action of mesenchymal stromal cells on hypoxia-induced pulmonary hypertension. *Circulation* 2012;126:2601–2611.
- 18 Zhu YG, Feng XM, Abbott J et al. Human mesenchymal stem cell microvesicles for treatment of Escherichia coli endotoxin-induced acute lung injury in mice. *Stem Cells* 2014;32:116–125.
- 19 Zhang B, Wang M, Gong A et al. HucMSC-exosome mediated-Wnt4 signaling is required for cutaneous wound healing. *Stem Cells* 2015;33:2158–2168.
- 20 Kordelas L, Rebmann V, Ludwig AK et al. MSC-derived exosomes: a novel tool to treat therapy-refractory graft-versus-host disease. *Leukemia* 2014;28:970–973.
- 21 Yoshioka S, Miura Y, Yao H et al. CCAAT/enhancer-binding protein β expressed by bone marrow mesenchymal stromal cells regulates early B-cell lymphopoiesis. *Stem Cells* 2014;32:730–740.
- 22 Sugino N, Miura Y, Yao H et al. Early osteoinductive human bone marrow mesenchymal stromal/stem cells support an enhanced hematopoietic cell expansion with altered chemotaxis- and adhesion-related gene expression profiles. *Biochem Biophys Res Commun* 2016;469:823–829.
- 23 Dominici M, Le Blanc K, Mueller I et al. Minimal criteria for defining multipotent mesenchymal stromal cells. The International Society for Cellular Therapy position statement. *Cytotherapy* 2006;8:315–317.
- 24 Yao H, Miura Y, Yoshioka S et al. Parathyroid hormone enhances hematopoietic expansion via upregulation of cadherin-11 in bone marrow mesenchymal stromal cells. *Stem Cells* 2014;32:2245–2255.
- 25 Iwasa M, Miura Y, Fujishiro A et al. Bortezomib interferes with adhesion of B cell precursor acute lymphoblastic leukemia cells through SPARC up-regulation in human bone marrow mesenchymal stromal/stem cells. *Int J Hematol* 2017;105:587–597.
- 26 Maas SL, De Vrij J and Broekman ML. Quantification and size-profiling of extracellular vesicles using tunable resistive pulse sensing. *J Vis Exp* 2014;92:e51623.
- 27 Murai M, Yoneyama H, Ezaki T et al. Peyer's patch is the essential site in initiating murine acute and lethal graft-versus-host reaction. *Nat Immunol* 2003;4:154–160.
- 28 Cooke KR, Kobzik L, Martin TR et al. An experimental model of idiopathic pneumonia syndrome after bone marrow transplantation: I. The roles of minor H antigens and endotoxin. *Blood* 1996;88:3230–3239.
- 29 Hill GR, Cooke KR, Teshima T et al. Interleukin-11 promotes T cell polarization and prevents acute graft-versus-host disease after allogeneic bone marrow transplantation. *J Clin Invest* 1998;102:115–123.
- 30 Wu H, Allan AE, and Harrist TJ. Noninfectious vesiculobullous and vesiculopustular diseases. In: Elder DE, ed. *Lever's Histopathology of the Skin*. 11th ed. Philadelphia, PA: Wolters Kluwer, 2015:315–317.
- 31 Takashima T, Kadowaki M, Aoyama K et al. The Wnt agonist R-spondin1 regulates systemic graft-versus-host disease by protecting intestinal stem cells. *J Exp Med* 2011;208:285–294.
- 32 Kanda Y. Investigation of the freely available easy-to-use software 'EZ' for medical statistics. *Bone Marrow Transplant* 2013;48:452–458.
- 33 Lötvall J, Hill AF, Hochberg F et al. Minimal experimental requirements for definition of extracellular vesicles and their functions: a position statement from the International Society for Extracellular Vesicles. *J Extracell Vesicles* 2014;3:26913.
- 34 Nakai W, Yoshida T, Diez D et al. A novel affinity-based method for the isolation of highly purified extracellular vesicles. *Sci Rep* 2016;6:33935.
- 35 Le Blanc K, Tammik L, Sundberg B et al. Mesenchymal stem cells inhibit and stimulate mixed lymphocyte cultures and mitogenic responses independently of the major histocompatibility complex. *Scand J Immunol* 2003;57:11–20.
- 36 Kaipe H, Erkers T, Sadeghi B et al. Stromal cells—are they really useful for GVHD? *Bone Marrow Transplant* 2014;49:737–743.
- 37 Hashmi S, Ahmed M, Murad MH et al. Survival after mesenchymal stromal cell therapy in steroid-refractory acute graft-versus-host disease: systematic review and meta-analysis. *Lancet Haematol* 2016;3:e45–e52.
- 38 Sugino N, Ichinohe T, Takaori-Kondo A et al. Pharmacological targeting of bone marrow mesenchymal stromal/stem cells for the treatment of hematological disorders. *Inflammation and Regeneration* 2017;37:7.
- 39 Kebriaei P, Isola L, Bahceci E et al. Adult human mesenchymal stem cells added to corticosteroid therapy for the treatment of acute graft-versus-host disease. *Biol Blood Marrow Transplant* 2009;15:804–811.
- 40 Arima N, Nakamura F, Fukunaga A et al. Single intra-arterial injection of mesenchymal stromal cells for treatment of steroid-refractory acute graft-versus-host disease: a pilot study. *Cytotherapy* 2010;12:265–268.
- 41 Di Nicola M, Carlo-Stella C, Magni M et al. Human bone marrow stromal cells suppress T-lymphocyte proliferation induced by cellular or nonspecific mitogenic stimuli. *Blood* 2002;99:3838–3843.
- 42 Tse WT, Pendleton JD, Beyer WM et al. Suppression of allogeneic T-cell proliferation by human marrow stromal cells: implications in transplantation. *Transplantation* 2003;75:389–397.
- 43 Maccario R, Podesta M, Moretta A et al. Interaction of human mesenchymal stem cells with cells involved in alloantigen-specific immune response favors the differentiation of CD4+ T-cell subsets expressing a regulatory/suppressive phenotype. *Haematologica* 2005;90:516–525.
- 44 Melief SM, Schrama E, Brugman MH et al. Multipotent stromal cells induce human regulatory T cells through a novel pathway involving skewing of monocytes toward anti-inflammatory macrophages. *Stem Cells* 2013;31:1980–1991.
- 45 Blazquez R, Sanchez-Margallo FM, de la Rosa O et al. Immunomodulatory potential of human adipose mesenchymal stem cells derived exosomes on in vitro stimulated T cells. *Front Immunol* 2014;5:556.
- 46 Conforti A, Scarsella M, Starc N et al. Microvesicles derived from mesenchymal

stromal cells are not as effective as their cellular counterpart in the ability to modulate immune responses in vitro. *Stem Cell Dev* 2014;23:2591–2599.

47 Gouveia de Andrade AV, Bertolino G, Riewaldt J et al. Extracellular vesicles secreted by bone marrow- and adipose tissue-derived mesenchymal stromal cells fail to suppress lymphocyte proliferation. *Stem Cells Dev* 2015;24:1374–1376.

48 Amarnath S, Foley JE, Farthing DE et al. Bone marrow-derived mesenchymal stromal cells harness purinergic signaling to tolerize human Th1 cells in vivo. *Stem Cells* 2015;33:1200–1212.

49 Kundrotas G. Surface markers distinguishing mesenchymal stem cells from fibroblasts. *Acta Medica Lituanica* 2012;19:75–79.

50 Prasad VK, Lucas KG, Kleiner GI et al. Efficacy and safety of ex vivo cultured adult human mesenchymal stem cells (Prochymal) in pediatric patients with severe refractory acute graft-versus-host disease in a compassionate use study. *Biol Blood Marrow Transplant* 2011;17:534–541.

51 Kurtzberg J, Prockop S, Teira P et al. Allogeneic human mesenchymal stem cell therapy (remestemcel-L, Prochymal) as a rescue agent for severe refractory acute graft-versus-host disease in pediatric patients. *Biol Blood Marrow Transplant* 2014;20:229–235.

52 Katsuda T, Kosaka N, Takeshita F et al. The therapeutic potential of mesenchymal stem cell-derived extracellular vesicles. *Proteomics* 2013;13:1637–1653.

53 Phinney DG, Di Giuseppe M, Njah J et al. Mesenchymal stem cells use extracellular

vesicles to outsource mitophagy and shuttle microRNAs. *Nat Commun* 2015;6:8472.

54 Glennie S, Soeiro I, Dyson PJ et al. Bone marrow mesenchymal stem cells induce division arrest anergy of activated T cells. *Blood* 2005;105:2821–2827.

55 Cuerquis J, Romieu-Mourez R, Francois M et al. Human mesenchymal stromal cells transiently increase cytokine production by activated T cells before suppressing T-cell proliferation: Effect of interferon-gamma and tumor necrosis factor-alpha stimulation. *Cytotherapy* 2014;16:191–202.

56 Ferrara JL, Cooke KR, and Teshima T. The pathophysiology of acute graft-versus-host disease. *Int J Hematol* 2003;78:181–187.

57 Sotiropoulou PA, Perez SA, Gritzapis AD et al. Interactions between human mesenchymal stem cells and natural killer cells. *Stem Cells* 2006;24:74–85.

58 Krampera M, Cosmi L, Angeli R et al. Role for interferon-gamma in the immunomodulatory activity of human bone marrow mesenchymal stem cells. *Stem Cells* 2006;24:386–398.

59 Itamura H, Shindo T, Tawara I et al. The MEK inhibitor trametinib separates murine graft-versus-host disease from graft-versus-tumor effects. *JCI Insight* 2016;1:e86331.

60 Jiang L, Huang Q, Zhang S et al. Hsa-miR-125a-3p and hsa-miR-125a-5p are downregulated in non-small cell lung cancer and have inverse effects on invasion and migration of lung cancer cells. *BMC Cancer* 2010;10:318.

61 Hashiguchi Y, Nishida N, Mimori K et al. Down-regulation of miR-125a-3p in human gastric cancer and its clinicopathological significance. *Int J Oncol* 2012;40:1477–1482.

62 Ninio-Many L, Grossman H, Shomron N et al. microRNA-125a-3p reduces cell proliferation and migration by targeting Fyn. *J Cell Sci* 2013;126:2867–2876.

63 Wang H, Peng W, Ouyang X et al. Circulating microRNAs as candidate biomarkers in patients with systemic lupus erythematosus. *Transl Res* 2012;160:198–206.

64 Zhao X, Tang Y, Qu B et al. MicroRNA-125a contributes to elevated inflammatory chemokine RANTES levels via targeting KLF13 in systemic lupus erythematosus. *Arthritis Rheum* 2010;62:3425–3435.

65 Collino F, Deregius MC, Bruno S et al. Microvesicles derived from adult human bone marrow and tissue specific mesenchymal stem cells shuttle selected pattern of miRNAs. *PLoS ONE* 2010;5:e11803.

66 Gauthier SD, Leboeuf D, Manuguerra-Gagné R et al. Stromal-Derived Factor-1α and Interleukin-7 Treatment Improves Homeostatic Proliferation of Naïve CD4(+) T Cells after Allogeneic Stem Cell Transplantation. *Biol Blood Marrow Transplant* 2015;21:1721–1731.

67 Ren G, Chen X, Dong F et al. Concise Review: mesenchymal stem cells and translational medicine: emerging issues. *Stem Cells Transl Med* 2012;1:51–58.

68 Lötvall J, Hill AF, Hochberg F et al. Minimal experimental requirements for definition of extracellular vesicles and their functions: a position statement from the International Society for Extracellular Vesicles. *J Extracell Vesicles* 2014;3:26913.

69 Zeringer E, Li M, Barta T et al. Methods for the extraction and RNA profiling of exosomes. *World J Methodol* 2013;3:11–18.



See www.StemCells.com for supporting information available online. STEM CELLS ; 00:000–000

Figure 1. Human BM-MSC-derived EVs suppress T cells and preserve naïve Treg *in vitro*.

Human PBMCs were activated with anti-CD3/CD28-coated Human T-Activator Dynabeads. These cells were cultured alone (black bars in A, C, F; *Control* in B, D, E, G), co-cultured with BM-MSCs (red bars in A, C, F; *BM-MSC* in B, D, E, G), or cultured with BM-MSC-derived EVs (purple bars in A, C, F; *EV* in B, D, E, G). (A) The number of viable cells was counted by Trypan blue dye exclusion. (B) Representative phase-contrast images of the cultures. Red arrows indicate PBMCs. Yellow arrows indicate Dynabeads. Bars, 50 μ m. Original magnification, $\times 200$. (C) Flow cytometric analysis showing the percentage of CD3⁺ T cells and the percentages of CD4⁺ and CD8⁺ T cells out of total CD3⁺ T cells. (D, E) Representative contour plots are shown. The numbers represent the percentage of CD3⁺ T cells or the percentages of CD4⁺ and CD8⁺ T cells out of total CD3⁺ T cells. The CD3-negative cell population, as determined by staining with isotype control antibodies, included few T cells (CD4⁺ or CD8⁺). (F, G) Flow cytometric analysis of three fractions of Foxp3-expressing cells, Fraction 1 (Fr1; CD45RA+Foxp3^{low} naïve Treg), Fraction 2 (Fr2; CD45RA-Foxp3^{high} activated Treg), and Fraction 3 (Fr3; CD45RA-Foxp3^{low} non-Treg). (F) The frequency of each Foxp3-expressing cell fraction out of total CD4⁺ T cells and the ratio of CD8⁺ T cells to each Foxp3-expressing cell fraction are shown. (G) Representative contour plots are shown. The numbers indicate the percentage of each fraction out of all CD4⁺ T cells. Data in (A, C, and F) represent the mean \pm SD. **, $P < 0.01$; *, $P < 0.05$.

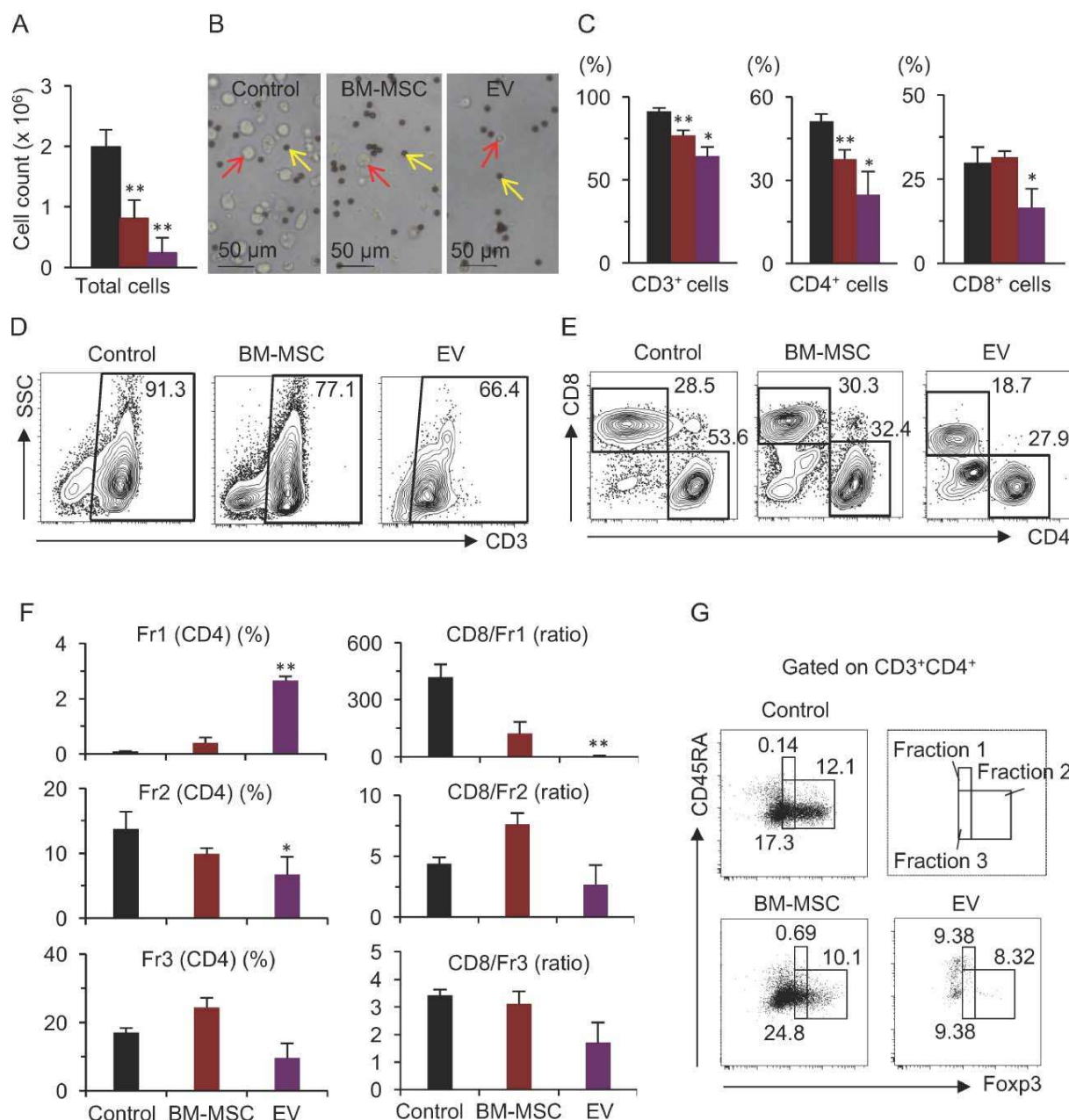


Figure 2. Human BM-MSC-derived EVs ameliorate the clinical and pathological characteristics of GVHD in mice.

(A) Schema of the EV treatment study. IR, irradiation; IV, intravenous infusion. (B) Survival curves of the GVHD mice that received human BM-MSC-derived EVs (*EV*, red line) or saline (*Control*, black line). The survival of the mice was observed until day 100 and plotted as a Kaplan–Meier curve ($n = 30$ for EV-treated GVHD mice; $n = 32$ for control GVHD mice). **, $P < 0.01$. (C) Clinical scores of the GVHD mice 10 days after the injection of spleen cells. Scores from five GVHD-associated parameters were summed, from 0 to 10 ($n = 28$ for EV-treated GVHD mice; $n = 18$ for control GVHD mice). (D) Histological scores of the GVHD mice. Scores from multiple GVHD-associated parameters were summed, from 0 to 28 for the large bowel and small bowel and from 0 to 40 for the liver ($n = 5$ for EV-treated GVHD mice; $n = 8$ for control GVHD mice). (E) Histological scores of seven parameters in the large bowel. (F) Representative microscopic images of hematoxylin and eosin-stained sections of large bowel specimens from the mice. Bars, 100 μm . Original magnification, $\times 100$. White and black bars in (C, D, and E) indicate the scores of GVHD mice that received BM-MSC-derived EVs (*EV*) or saline (*Control*). (G) Histological evaluation of skin specimens from the GVHD mice. The percentage of mice whose severity of damage was evaluated as moderate (black) or severe (white) is shown ($n = 5$ for EV-treated GVHD mice; $n = 9$ for control GVHD mice). In (D, E, and G), the scores were assessed 6 days after the administration of EVs. Data in (C–E) indicate the mean \pm SD. **, $P < 0.01$; *, $P < 0.05$.

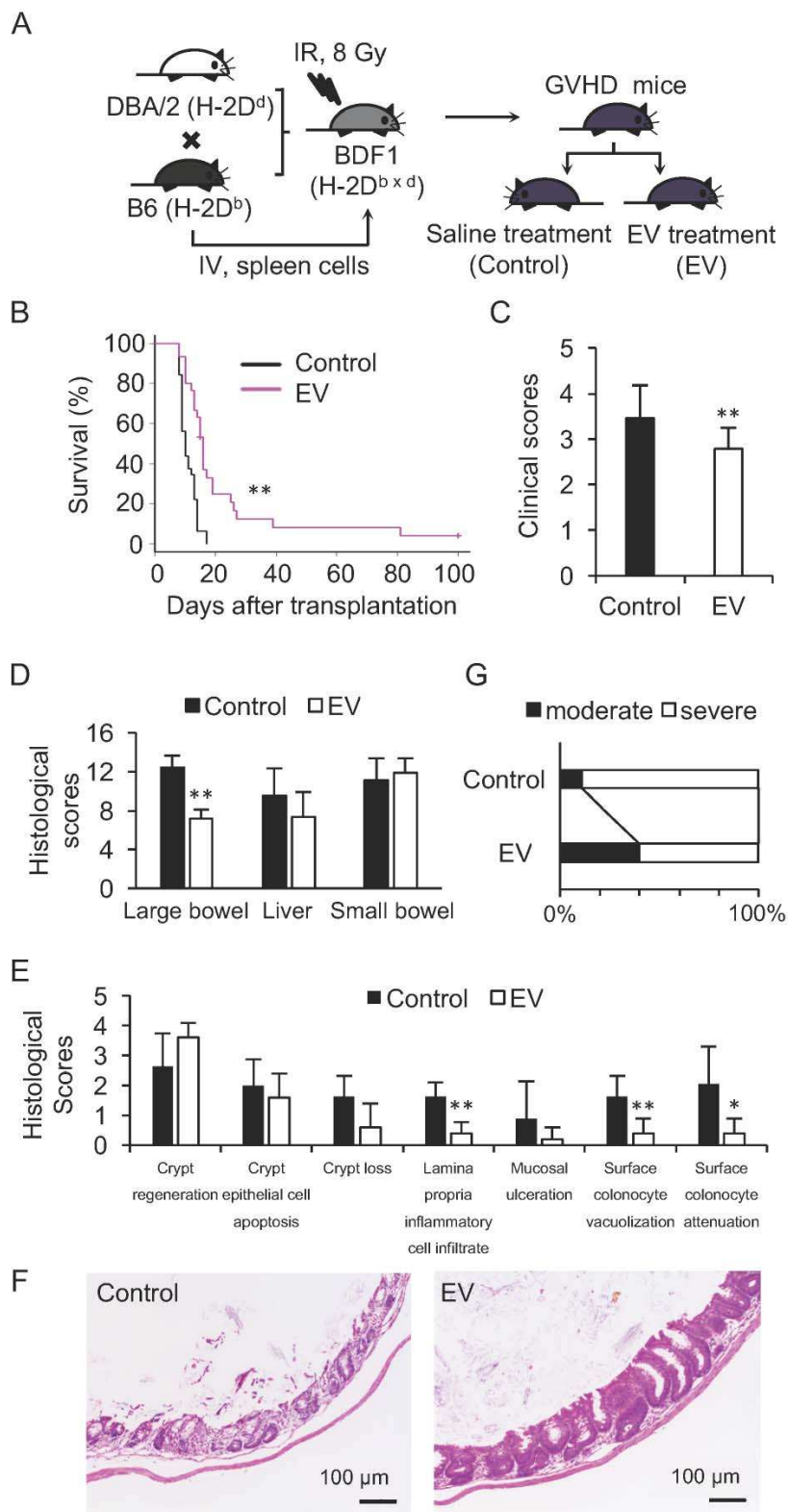


Figure 3. Human BM-MSC-derived EVs preserve peripheral naive T cells and Treg in mice with GVHD.

Flow cytometric analysis of T cell subsets in PB from the GVHD mice 6 days after the administration of EVs. (A) The frequency of CD8+ and CD4+ T cells. (B) Representative contour plots are shown. (C) The frequency of naive (Tn; CD62L+CD44-), effector (Teff; CD62L-CD44+), and central memory and effector memory (Tcm and Tem; CD62L+CD44+) T cells out of total CD8+ and CD4+ T cells. (D) Flow cytometric analysis of Treg. The numbers indicate the percentage of Treg out of total CD4+ T cells in the PB. No GVHD, BDF1 mice that did not receive spleen cells from B6 mice; Control GVHD, BDF1 mice that received spleen cells from B6 mice (H-2D^b) but did not receive human BM-MSC-derived EVs; EV-treated GVHD, BDF1 mice that received spleen cells from B6 mice and then received human BM-MSC-derived EVs. Data in (A, C) indicate the mean \pm SD. **, $P < 0.01$; *, $P < 0.05$.

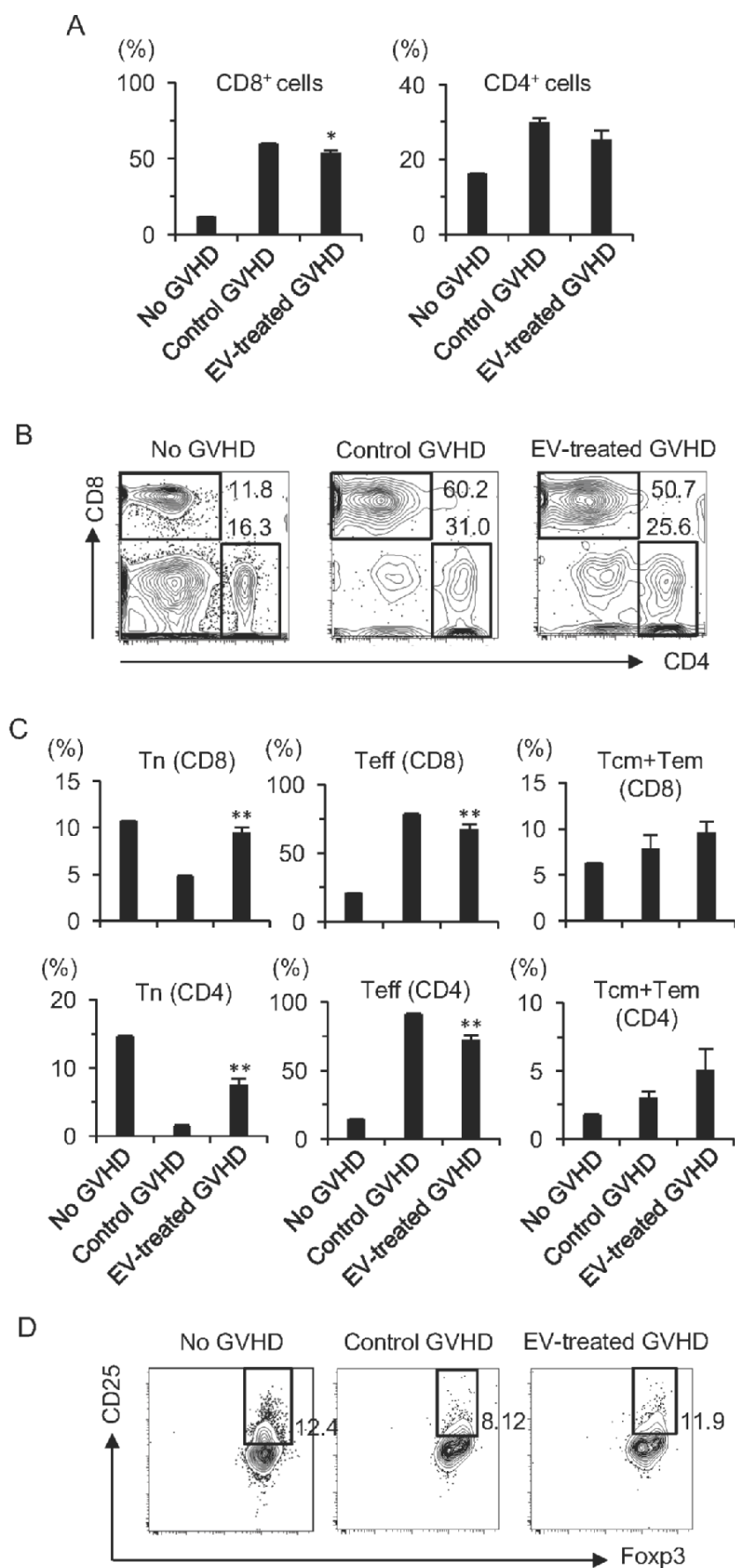
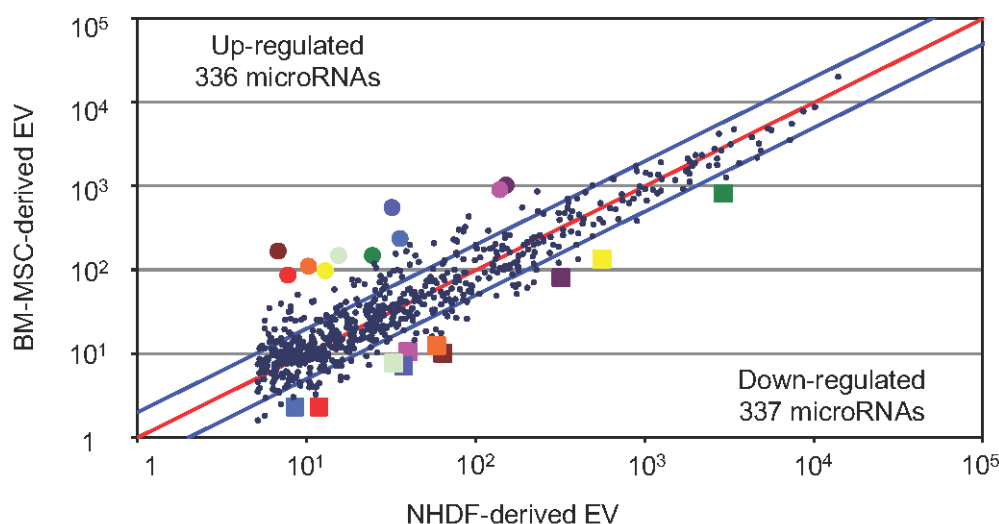


Figure 4. Microarray analysis of microRNAs in BM-MSC-derived EVs versus NHDF-derived EVs.

(A) Scatter plot of microRNAs expressed in BM-MSC-derived EVs compared with NHDF-derived EVs. Blue lines indicate the 2.0-fold threshold. Circles represent the top ten up-regulated microRNAs in BM-MSC-derived EVs. Squares represent the top ten down-regulated microRNAs in BM-MSC-derived EVs. (B) List of the top ten microRNAs that were up- or down-regulated in BM-MSC-derived EVs. The color of the numbers corresponds to the color of the circles or squares in the scatter plot in (A). (C) KEGG pathway analysis of mRNAs that were commonly targeted by three or more microRNAs among the top ten up- or down-regulated microRNAs.

A**B**

Up-regulated				Down-regulated			
	Name of microRNA	Ratio (Log2)	Target mRNA (number)		Name of microRNA	Ratio (Log2)	Target mRNA (number)
①	hsa-miR-125a-3p	4.61	4649	1	hsa-miR-3687	-2.68	643
②	hsa-miR-4732-5p	4.10	2592	2	hsa-miR-4465	-2.40	1042
③	hsa-miR-143-3p	3.48	487	3	hsa-miR-1273h-5p	-2.36	6956
④	hsa-miR-1249-5p	3.43	5506	4	hsa-miR-3194-3p	-2.26	5019
⑤	hsa-miR-145-5p	3.25	891	5	hsa-miR-4531	-2.09	5298
⑥	hsa-let-7d-5p	2.91	1191	6	hsa-miR-4525	-2.06	4324
⑦	hsa-miR-1246	2.76	3043	7	hsa-miR-4638-5p	-2.01	2010
⑧	hsa-miR-4741	2.72	4549	8	hsa-miR-451a	-1.93	28
⑨	hsa-miR-21-5p	2.70	382	9	hsa-miR-330-3p	-1.91	1024
⑩	hsa-let-7a-5p	2.58	1191	10	hsa-miR-4749-5p	-1.84	1607

C

KEGG map number	Gene group (Genes number included)	Corrected <i>p</i> -value	microRNA
04110	Cell cycle (26)	9.87E-05	Up-regulated
04660	T cell receptor signaling pathway (29)	5.96E-06	Up-regulated
05332	Graft-versus-host disease (4)	4.51E-03	Up-regulated

Table 1. List of enriched GO terms. GO analysis of commonly targeted genes by up- or down-regulated microRNAs in BM-MSC-derived EVs.

GO accession	GO term (number of genes included)	Corrected <i>P</i> -value	microRNA
0008284	Positive regulation of cell proliferation (93)	4.20E-16	Up-regulated
0008285	Negative regulation of cell proliferation (86)	2.28E-09	Down-regulated
0007049	Cell cycle (79)	2.49E-06	Up-regulated
0008283	Cell proliferation (64)	5.82E-07	Up-regulated
0051301	Cell division (47)	2.11E-03	Up-regulated
0000278	Mitotic cell cycle (43)	1.39E-02	Up-regulated
0000082	G1/S transition of mitotic cell cycle (29)	1.49E-03	Up-regulated
0007067	Mitosis (29)	1.42E-02	Up-regulated
0007050	Cell cycle arrest (28)	6.70E-03	Down-regulated
0030307	Positive regulation of cell growth (13)	6.91E-03	Up-regulated
0051781	Positive regulation of cell division (13)	2.43E-03	Up-regulated
0045786	Negative regulation of cell cycle (11)	1.48E-02	Down-regulated
0045787	Positive regulation of cell cycle (8)	8.83E-03	Up-regulated
0045930	Negative regulation of mitotic cell cycle (5)	4.67E-02	Down-regulated
0071158	Positive regulation of cell cycle arrest (5)	3.04E-02	Down-regulated

Graphical Abstract

Systemic infusion of human BM-MSC-derived EVs prolongs the survival of mice with GVHD and reduces the clinical symptoms and pathologic damage in multiple GVHD-targeted organs. CD4⁺CD25⁺Foxp3⁺ regulatory T cells and CD62L⁺CD44⁻ naive T cells are preserved in peripheral blood of GVHD mice treated with BM-MSC-derived EVs. Microarray analysis of microRNAs in BM-MSC-derived EVs shows up-regulation of miR-125a-3p and down-regulation of cell proliferative processes, as identified by Gene Ontology enrichment analysis.

